Ab initio model potential study of local distortions around Cr^+ and Cr^{3+} defects in fluorite

Luis Seijo[a] and Zoila Barandiarán[a]
Departamento de Química Física Aplicada, C-14, Universidad Autónoma de Madrid, 28049 Madrid, Spain

(Received 3 January 1991; accepted 4 March 1991)

In this paper we present the results of a theoretical study of the local geometry distortions produced by Cr^+ and Cr^{3+} ions in fluorite, by means of the *ab initio* environment model potential method [J. Chem. Phys. **89**, 5739 (1988)]. The valence energy and wave function of the $(CrF_8)^{q-}$ $(q=7,5)$ clusters embedded in the CaF_2 lattice represented by 118 *ab initio* model potential ions plus 750 point-charge ions are calculated using a short CI, which includes all states related to the d^n ionic configuration. A geometry optimization is performed for $CaF_2:(CrF_8)^{7-}$ within the cubic point symmetry and for $CaF_2:(CrF_8)^{5-}$ within the D_{3d} point symmetry; the conclusions of analyses of the multimode Jahn–Teller coupling $T_1 \otimes (\epsilon + \tau_2 + \tau_2')$ are used to address the geometry optimization, which is completed by a final unrestricted search. In an attempt to study all the structures proposed along previous experimental studies, the D_{3d} structure corresponding to an octahedral cluster plus two axially displaced fluorines (octahedron + 2) is investigated. Taking the ground state energy of the perfect cube as a reference, the results show that the most stable D_{3d} distortion corresponds to an elongated cube in a $^4A_{2g}$ ground state, with an energy of about $-1700\ cm^{-1}$, while the compressed cube and the octahedron + 2 structure energies are found to be -780 and $+40\,000\ cm^{-1}$, respectively. A joint analysis of the available experimental data and the results of our calculations are presented.

I. INTRODUCTION

The knowledge of the local distortion produced in a perfect crystal by the presence of an impurity is considered to be of paramount importance from various points of view: On the one hand, it is a key factor for the theoretical study of other geometry dependent properties following an *ab initio* procedure. On the other hand, it is very often necessary for a correct interpretation of experimental results. From the experimental point of view, however, the measurement of the local geometry parameters is a very difficult target[1] and its qualitative nature is usually indirectly deduced.[2–5] Under these circumstances, *ab initio* theoretical studies which predict local geometry distortions should be very valuable. Particularly, the confluence of complementary information (experimental data and theoretical predictions) should facilitate the understanding of the electronic properties of such complex systems. Here, we present the results of an *ab initio* theoretical investigation of the local geometry distortions produced by Cr^+ and Cr^{3+} defects in fluorite. In this way, the available experimental information, from which no definite conclusions can be drawn as to what is the geometry around the defects, is complemented.

Fluorite and crystals with fluorite structure are host to transition metal ions providing an eightfold cubic coordination. These systems add to their intrinsic interest[2] the fact that they constitute *ideal* cases, whose knowledge can provide a better understanding of the properties of the transition metal ions in crystals such as $BeAl_2O_4$, which show more technological interest but also more complexity.[5] Although the amount of experimental work on the eightfold coordination is not as large as in the case of lower coordinations, it is abundant and it has been reviewed.[2] On the contrary, we are not aware of the existence of *ab initio* theoretical studies on transition metal impurities in eightfold coordination.

Fluorite and fluoritelike crystals with Cr^{3+} impurities have been experimentally studied by means of electron paramagnetic resonance (EPR)[2–4,6,7] as well as optical absorption[5,7,8] and emission[5] spectroscopies. The Cr^+ impurity has been observed in Cr^{2+} doped samples after X irradiation, which actually creates both Cr^+ and Cr^{3+} defects.[4] While there seems to be no doubt that the Cr^+ ion has a cubic coordination,[4] it is not so clear what the local environment of Cr^{3+} impurities is. In effect, it is agreed that the local symmetry around Cr^{3+} is D_{3d}, but EPR measurements have been interpreted as due to both (i) a D_{3d} compressed cube originated by a Jahn–Teller coupling between the $^4T_{1g}$ ground state of Cr^{3+} in eightfold cubic coordination and the two τ_{2g} modes of CrF_8,[3] and (ii) a D_{3d} elongated cube resulting from the same Jahn–Teller coupling,[4] this one leading to different final arrangements around Cr^{3+}: a distorted octahedron in CaF_2 and a distorted cube in SrF_2. In addition, the optical absorption properties of Cr^{3+} doped fluoritelike crystals have been interpreted as due to a very large relaxation (hardly due to a quadratic Jahn–Teller coupling) along which six fluorines form a nearly perfect octahedron around Cr^{3+} and the other two fluorines move away along a C_3 axis going beyond their perfect lattice sites and creating a very small trigonal field.[5,7] However, in order to interpret the special features of the emission spectra (very large

[a] (E-mail: ARTI@EMDUAM11.BITNET).

 0021-9606/91/128158-07$03.00

Stokes shift and very low emission quenching temperatures) with such a model for the geometry of the ground state, it has been found necessary to accept a nearly eightfold cubic coordination for the excited state.

The interpretation of the experimental data leads, as we have just summarized, to three possible D_{3d} arrangements around the Cr^{3+} impurity in fluoritelike crystals; we have studied their relative stability by means of the application of the *ab initio* environment model potential method,[9,10] to the $(CrF_8)^{5-}$ cluster embedded in CaF_2. In this way, we try to provide some additional insight into the nature of the Cr^{3+} defects. The results of this theoretical investigation are presented here together with those corresponding to the local geometry optimization around the Cr^+ defect.

In Sec. II we present a brief outline of the method together with the details of the calculations. In Sec. III we present the results of the calculations, which, for the Cr^{3+} defect, lead to a D_{3d} Jahn–Teller elongated cube on a $^4A_{2g}$ ground state as the most stable structure; a discussion is presented which shows that such a structure is compatible with the experimental information gathered up to now.

II. METHOD

The *ab initio* environment model potential method used to perform the embedded cluster calculations has been presented in Refs. 9 and 10; here we will only summarize its main features. The method is a practical means to apply to imperfect crystals the theory of separability of many-electron systems,[11–13] from which the basic assumptions and equations are taken. First, the imperfect crystal is arbitrarily divided into a cluster (usually including the defect and its nearest neighbors) and environment groups A, B,..., and a normalized antisymmetric product wave function is adopted for the imperfect crystalline system:

$$\Psi^{\text{crys}} = \hat{MA}\,[\Phi^{\text{clus}}\Phi^A\Phi^B\cdots], \tag{1}$$

where the Φ's are antisymmetric (mono- or multiconfigurational) group wave functions representing, respectively, the electrons of the cluster and of the environment groups. Then, if the group wave functions are strong orthogonal,[11] the total energy of the crystal can be expressed as

$$E = E_{\text{clus}} + E_{\text{clus-env}} + E_{\text{env}}, \tag{2}$$

and the variational treatment of the cluster embedded in a frozen environment leads to the equations for the optimum Φ^{clus} and $E_{\text{clus}} + E_{\text{clus-env}}$.[12] This is the first step of a building block technique in which the variational treatment is successively and iteratively applied to the cluster and the environment groups. When this procedure is fully applied, the result is a cluster embedded in a polarized environment. If only the first step is given, the cluster is embedded in a frozen environment.

The practical application of this theory demands the calculation of cumbersome interactions between cluster and environment which are involved in $E_{\text{clus-env}}$. They are approximated following the ideas of the *ab initio* core model potential method,[14–16] so that model potentials representing the true environment potentials acting on the cluster are obtained directly from the wave functions of the environment groups (cations and anions in this case) Φ^A, Φ^B, etc., without the use of any parametrization procedure. The environment model potentials *explicitly* include the long-range and short-range Coulomb interactions, the quantum exchange interactions, and the quantum orthogonality interactions.

A. Details of the calculations

Chromium ions in fluorite occupy cation substitutional positions (see Fig. 1) with eightfold coordination. In this study, the cluster [Eq. (1)] is arbitrarily defined as the $(CrF_8)^{q-}$ unit ($q = 7$ for the Cr^+ defect and $q = 5$ for the Cr^{3+} defect) and the environment groups are the remaining Ca^{2+} and F^- ions. Previous numerical experimentation[9] has revealed that convergence of the cluster energy with the environment size in ionic crystals is very efficiently achieved if the environment groups are arranged by *shells* defined so that the nth shell includes the lattice sites between two concentric cubic volumes whose edge lengths are na_0 and $(n+1)a_0$ and which are centered on the impurity. Following this approach, it has been found[9] that the results reach the required convergence with a lattice model including one external shell of complete-ion model potentials (both for cations and anions) plus two shells of point-charge ions (using fractional charges for the frontier ions[17]). We have used such a lattice model to define the cluster environment: The first shell includes 118 *ab initio* model potential ions surrounding the cluster (it is shown in Fig. 1); The second and third shells include the next 750 ions. In all cases, the lattice sites have been taken from the experimental crystal structure of fluorite.[18] The complete-cation (Ca^{2+}) and complete-anion (F^-) *ab initio* model potentials, which are available from the authors upon request, have been obtained from the Hartree–Fock–Roothan wave functions of Ca^{2+} and F^- ions embedded in the CaF_2 lattice: Ca^{2+} (33111/3111) and F^- (3111/111) basis sets[19] have been used in the calculation of the embedded Ca^{2+} and F^- ions, respectively; the calculations have been repeated until self-consistency

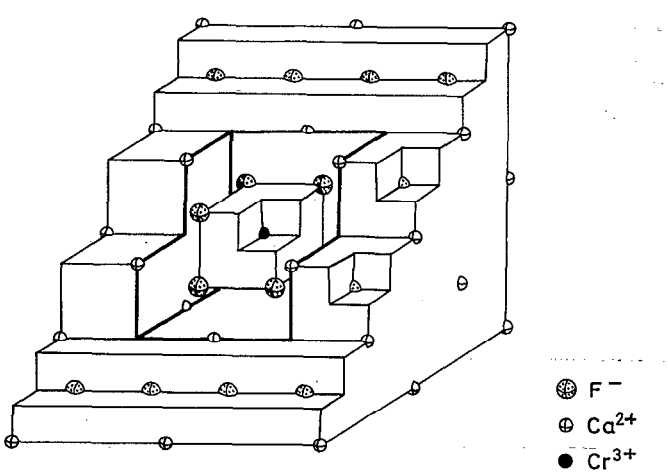

FIG. 1. Cross section of the $(CrF_8)^{q-}$ cluster and the first environment shell of 118 *ab initio* model potential ions.

between the CaF_2 lattice group wave functions (which generate the environment model potentials) and the Ca^{2+} and F^- embedded ion wave functions has been accomplished.[20]

We have performed quantum mechanical calculations on the embedded clusters $(CrF_8)^{7-}$ and $(CrF_8)^{5-}$. In order to reduce the size of the computations with an acceptable loss of precision, we have adopted the *ab initio* core model potential approximation[14–16] for chromium and fluorine. A Mg-like frozen core has been used for chromium with a $(81/321^*/3111^d)$ valence basis set,[15] which includes an extra d-diffuse function.[21] A He-like frozen core has been used for fluorine with a $(41/411^d)$ valence basis set,[14] which includes a p-diffuse function for the anion.[22]

The embedded cluster $(CrF_8)^{7-}$ with cubic symmetry has a ${}^6A_{1g}$ ground state, whose valence energy and wave function have been calculated at the monoconfigurational level $(e_g^2 t_{2g}^3 - {}^6A_{1g})$ using the restricted open-shell Hartree–Fock–Roothan (ROHF) equations of Ref. 23. We have optimized its energy with respect to the Cr–F distance.

The cluster $(CrF_8)^{5-}$ with cubic symmetry shows a ${}^4T_{1g}$ electronic ground state which undergoes a multimode Jahn–Teller coupling with the doubly degenerate ϵ_{2g} vibrational mode and the two triply degenerate τ_{2g} vibrational modes of the CrF_8 unit, $T_1 \otimes (\epsilon + \tau_2 + \tau_2')$.[24,25] This could lead to either tetragonal, trigonal, or intermediate distortions. The competition between the $T_1 \otimes \epsilon$ and $T_1 \otimes \tau_2$ vibronic couplings has been discussed (see Ref. 24 and references therein) for different types of coordinations and it has been suggested that trigonal distortions should be more effective in eightfold coordination than tetragonal ones.[24,25] This conclusion coincides with the experimentally accepted D_{3d} local symmetry for the Cr^{3+} defect.[2,4,5] Accordingly, we have only examined the D_{3d} structures. The search for energy minima may be simplified on the basis of the analysis of the quadratic (first order) Jahn–Teller approximation:[26] The D_{3d} symmetry corresponds to a vibronic coupling with the two τ_{2g} modes, $T_1 \otimes (\tau_2 + \tau_2')$, and the condition for a structure to be a minimum imposes a relationship between the three τ_{2g} coordinates, on the one hand, and between the three τ_{2g}' coordinates, on the other, reducing the number of degrees of freedom to two. Consequently, the geometry optimization procedure that we have adopted has been the following: First, the ground state energy has been optimized within the cubic symmetry. Then, taking the optimized cube as the reference, a search for minima has been performed within the two-dimensional energy surface defined by two nuclear motion coordinates Ω and Ω' (see the Appendix,) which correspond to coupled displacements of the fluorine nuclei from their cubic equilibrium sites, producing a D_{3d} symmetry. Finally, the structure of minimal energy within that surface has been relaxed by allowing the most distant fluorines move independently.

We have adopted for the $(CrF_8)^{7-}$ cluster a configuration interaction wave function which includes all the states related to the $3d^3$ configuration of Cr^{3+} which we call d^n–CI and which is the smallest meaningful wave function for these kind of open-shell systems. A much larger CI would be required for the calculation of absorption and emission spectra, as has been shown by Shaskin and Goddard in K_2CuF_4:$(CuF_6)^{4-}$ (Ref. 27); however, the nature of the equilibrium structures is expected to be well reproduced with the simpler wave function used here, which, on the other hand, makes the geometry optimization affordable. Within the cubic symmetry, the ${}^4T_{1g}$ ground state is a mixture of two configuration states: $e_g^2 t_{2g}$ and $e_g t_{2g}^2$. Within D_{3d} symmetry, the e_g orbitals remain degenerate, whereas the three t_{2g} orbitals split into a_{1g} and e_g orbitals (which we will call e_g'); also, the ${}^4T_{1g}$ state splits into a ${}^4A_{2g}$ and a ${}^4E_g$ which alternatively become the ground states in different regions of the D_{3d} energy surface. The ${}^4A_{2g}$ state is a mixture of the $e_g^2 a_{1g}$, $e_g a_{1g} e_g'$, and $a_{1g} e_g'^2$, configurations and the corresponding d^n–CI matrix has been generated from the single-reference $e_g^2 a_{1g}$–${}^4A_{2g}$ ROHF calculation.[23] The ${}^4E_g$ state is a mixture of $e_g^2 e_g'$, $e_g a_{1g} e_g'$, and $e_g e_g'^2$, and the corresponding matrix has been generated from the $e_g^2 e_g'$–${}^4E_g$ ROHF calculation,[23] which allows the occupation of two open shells of the same symmetry.

III. RESULTS AND DISCUSION

A stationary point has been found for the $(CrF_8)^{7-}$ cluster on its ${}^6A_{1g}$ cubic ground state at $R(Cr–F) = 2.49$ Å, which means an increase over the bulk Ca–F distance (2.37 Å) by 0.1 Å. For the $(CrF_8)^{5-}$ cluster on its ${}^4T_{1g}$ cubic ground state, the minimum of the breathing mode lies at $R(Cr–F) = 2.11$ Å, 0.26 Å shorter than the bulk Ca–F distance. This is not, however, a stationary point. Taking it as a reference for distortions (Jahn–Teller-like), two minima have been found in the (Ω, Ω') D_{3d} surface (see the Appendix). The most stable minimum corresponds to the ${}^4A_{2g}$ state and lies 1700 cm^{-1} below the cubic reference; it is located at $\Omega = 0.461$ a.u. and $\Omega' = -0.170$ a.u., which, in terms of the geometry parameters defined in Fig. 2, corresponds to a D_{3d} elongated cube with $R(Cr–F_1) = 2.26$ Å,

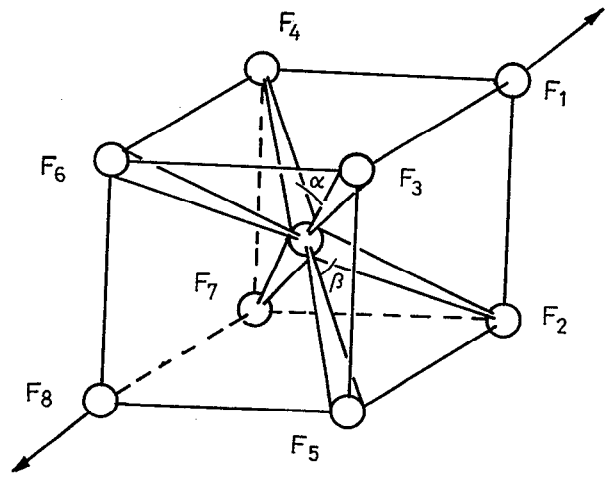

FIG. 2. The $(CrF_8)^{5-}$ cluster. F_1 and F_8 move along the C_3 axis. F_2 to F_7 move under a D_{3d} symmetry constraint: $R(Cr–F_2)$ and α are *independent* geometry parameters.

TABLE I. D_{3d} structures of $CaF_2:(CrF_8)^-$. The geometry parameters correspond to Fig. 2.

Structure	State	Geometry parameters				$[E-E_0(^4T_{1g})]$ (cm^{-1})
		R(Cr–F_1)(Å)	R(Cr–F_2)(Å)	α(deg)	β(deg)	
JT elongated	$^4A_{2g}$	2.26	2.06	108	72	−1 700
JT compressed	^4E_g	2.02	2.14	110	70	−780
Octahedron + 2	$^4A_{2g}$	2.84	1.88	90	90	+46 000
Perfect cube				109.47	70.53	

R(Cr–F_2) = 2.06 Å, and $\alpha = 108°$ ($\beta = 72°$) (see Table I). The position of the axial fluorines F_1 and F_8 have been further optimized, but they stayed unchanged within the fitting errors. The second minimum corresponds to a ^4E_g ground state and lies 780 cm^{-1} below the cubic reference; it is located at $\Omega = -0.255$ a.u. and $\Omega' = 0.036$ a.u., which corresponds to a D_{3d} compressed cube with R(Cr–F_1) = 2.02 Å, R(Cr–F_2) = 2.14 Å, and $\alpha = 110°$ ($\beta = 70°$) (Table I). This state suffers an additional Jahn–Teller distortion, which has not been explored in this work.

In order to study the structure proposed in Refs. 5 and 7 for the Cr^{3+} defect corresponding to a perfect octahedron of fluorines plus two axially displaced fluorines, a region of the D_{3d} surface has been explored under the constraint $\alpha = 90°$ ($\beta = 90°$). The most stable structure of this kind (octahedron + 2 in Table I) corresponds to R(Cr–F_1) = 2.84 Å and R(Cr–F_2) = 1.88 Å, its energy being 46 000 cm^{-1} *above* the cubic reference. This point does not belong to the D_{3d} (Ω, Ω') surface, but, in order to compare the relative distortions, we can say that a point within this surface with $\alpha = 90°$ and R(Cr–F_2) = 1.88 Å [with corresponding R(Cr–F_1) = 3.00 Å], would lie around $\Omega = 2.7$ a.u., $\Omega' = -2.4$ a.u., very far away from the regions of the $^4A_{2g}$ and ^4E_g minima described above.

Before getting into the analysis of all the information gathered so far, joining the available experimental data and our own results, some remarks can be helpful. The first one is related to the residual uncertainties of our results; the second one is related to the matching between the defects modeled by our calculations and the defects actually present in the measured samples. In effect, the consideration of correlation effects beyond the d^n–CI used here and of lattice relaxation should improve the quality of our predictions for the equilibrium bond lengths and angles as well as for the relative stability of the structures investigated. Nevertheless, these methodological improvements are not expected to change considerably the calculated geometrical parameters nor to change qualitatively the relative stability of the structures examined: This is particularly so in the case of the octahedron + 2 vs the JT-distorted structures (Table I).

The second aspect to keep in mind along a joint analysis of experimental and theoretical results is the following: Chan and Shields[6] have pointed out that different mechanisms for the excess charge compensation in chromium doped fluoritelike crystals may occur; this leading to different types of Cr^{3+} defects, not all of which, as we see next, should be comparable with the defects modeled by our calculations. It has been pointed out that local excess charge compensation may be achieved through the presence of either interstitial fluoride (favored when the crystal is grown in a fluorine atmosphere) or substitutional oxide (through decomposition of impurity content of water). A different (nonlocal) mechanism has been described for samples of Cr^{2+} doped crystals by Alcalá *et al.*[4] Here, the Cr^{3+} and Cr^+ defects are produced in the same concentration by X irradiation of the Cr^{2+} doped sample thus being each type of center the nonlocal charge compensator of the other [they are shown to be distant enough from each other by the superhyperfine structure of the EPR spectra at different orientations of the magnetic field which reveals a D_{3d} (not C_{3v}) local symmetry]. Obviously, the model used in our investigation should represent the Cr^{3+} defects with nonlocal charge compensation and different models should be used to study Cr^{3+} defects with interstitial fluoride or substitutional oxide charge compensators. We can expect from this that our calculations correspond to the Cr^{3+} defect observed in Ref. 4. In Refs. 5 and 7, the nature of the charge compensators is not so clear, therefore the defects studied would correspond to our model as long as the local mechanisms through interstitial or substitutional ions can be ruled out.

With the previous remarks in mind, we can say that the results of our calculations support the conclusions of Ref. 4 about the local geometry of the Cr^{3+} defect: It corresponds, essentially, to a D_{3d} JT-elongated distortion of the cube. In the model adopted in Ref. 4 for the distortion in CaF_2 and SrF_2 (which corresponds to the Jahn–Teller coupling with only one τ_{2g} mode), fluorines 2, 3, and 4 (Fig. 2) move towards the cubic position of F_1 along the cubic edges (F_5, F_6, and F_7 move correspondingly towards the cubic position of F_8); our results predict, however, a distortion along which fluorines 2 to 7 move essentially towards chromium, with only a small increase of β. We obtain $\beta = 72°$, slightly larger than the perfect cube value, 70.53°. This is quite smaller than the value estimated by Alcalá *et al.*[4] in CaF_2, 85° ± 4°, which becomes 78° ± 4° in SrF_2.

The D_{3d} JT-compressed structure proposed by Zaripov *et al.*[3] results less stable in our calculations. It is to be noted that such structure has been proposed in order to interpret EPR measurements on crystals grown in a fluorine atmosphere, so that interstitial fluorine ions might be present, creating other than the defect studied in the present calculation.

Finally, Borcherts and Lohr,[7] as well as Payne *et al.*,[5] have proposed a structure for the ground state of $(CrF_8)^{5-}$ which is a perfect or almost perfect octahedron of fluorines, plus two axially displaced fluorines. This structure is definitely not supported by our calculations for a Cr^{3+} defect with nonlocal charge compensation (i.e., excluding interstitial or substitutional charge compensator ions). The octahedron + 2 structure has been proposed in order to interpret the existence of only two broad bands in Cr^{3+} doped fluorite and fluoritelike crystals,[5,7] which have been assigned to the transitions $^4A_{2g} \rightarrow {}^4T_{2g}$ and $^4A_{2g} \rightarrow a\,{}^4T_{1g}$ (Fig. 3) between *octahedral* electronic states (a third band assigned to $^4A_{2g} \rightarrow b\,{}^4T_{1g}$ has been observed in CaF_2 and CdF_2). The first of these bands in CdF_2 consists of two overlapping bands separated 725 cm^{-1},[7] which have been associated to the splitting of the octahedral $^4T_{2g}$ arising from the residual trigonal field (Fig. 3). However, the second band has not been observed to be analogously split. Furthermore, in CaF_2, SrF_2, and BaF_2 only the *first* band shows clearly a complex structure.[5] Finally, the emission spectra of these systems show peculiar characteristics which cannot be explained if the octahedron + 2 structure is maintained upon the electronic transition: unusually large Stokes shifts and low emission quenching temperatures, compared with other octahedral systems such as $K_2NaGaF_6:Cr^{3+}$. In order to make this compatible with the octahedron + 2 structure proposed for the ground state, a nearly eightfold cubic coordination has been proposed for the equilibrium geometry of the first excited state.[5]

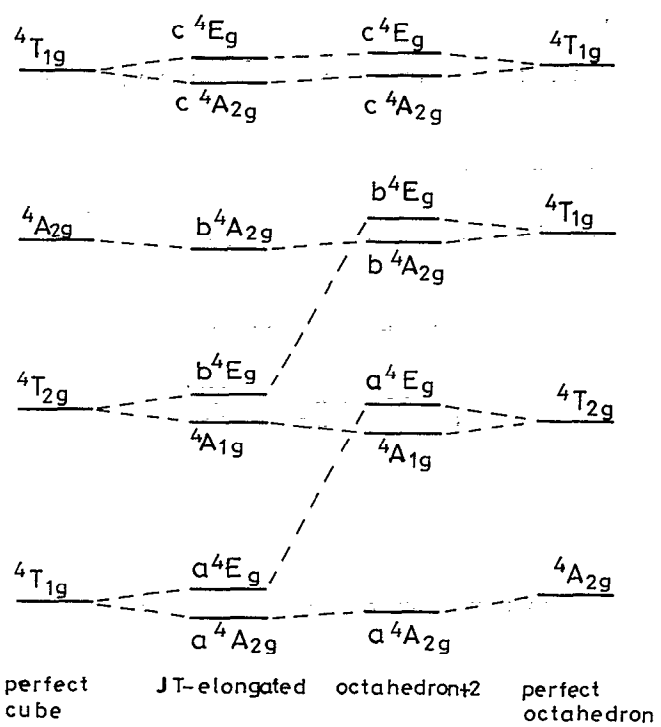

FIG. 3. Qualitative correlation diagram of the states of the $(CrF_8)^{5-}$ cluster corresponding to various structures. The Jahn–Teller-elongated and octahedron + 2 structures have D_{3d} symmetry. See the text for details.

The *ab initio* study of the previous spectral features requires the calculation of the energy hypersurface of some excited states, as well as the calculation of the absorption and emission spectra from the corresponding equilibrium geometries using large CI. This is not a simple task and will be the subject of further studies. However, we would only like to point out here that a JT-elongated structure for the ground state like the one predicted here is compatible not only with the features of the EPR spectrum, but also with those of the optical absorption/emission spectra. To show this we will bring together our prediction for the Jahn–Teller energy of the $^4A_{2g}$ ground state, 1700 cm^{-1}, and the experimental value for the splitting of the cubic $^4T_{2g}$ into $^4A_{1g}$ and $b\,{}^4E_g$ at the equilibrium geometry of the ground state, 725 cm^{-1}[7] (see Fig. 4). In effect, the assignment of the first and second absorption bands to $^4A_{2g} \rightarrow {}^4A_{1g}$, $b\,{}^4E_g$ and $\rightarrow b\,{}^4A_{2g}$, would agree with the fact that the first is a complex band while the second seems to be a simple one (see Fig. 3: JT elongated and Fig. 4). Also, if the splitting of the cubic $^4T_{1g}$ ground state is not large, the band $^4A_{2g} \rightarrow a\,{}^4E_g$ could have remained hidden to the optical measurements, since, to our knowledge, none of them seems to have explored the region below 3000 cm^{-1}; we obtain 2200 cm^{-1} for this splitting and, although it should not be taken quantitatively since its reliable calculation requires larger CI, a value close to it could be plausible if one accepts that the splitting of the cubic $^4T_{2g}$ state at the equilibrium geometry of the ground state is only 725 cm^{-1} [the splitting of the first absorption band in CdF_2 (Ref. 7)]. Moreover, the unusually large Stokes shifts are also consistent with the JT-elongated structure. In effect, the Stokes shifts of the D_{3d} states have two contributions: one is due to the relative shift of the cubic states $^4T_{1g}$ and $^4T_{2g}$ whose minima are the respective origins for their D_{3d} distortions; the second is due to the relative shift in the D_{3d} distortion coordinate space, which is not present in the case of perfect octahedra such as $K_2NaGaF_6:Cr^{3+}$. A large value for the second contribution is compatible with a Jahn–

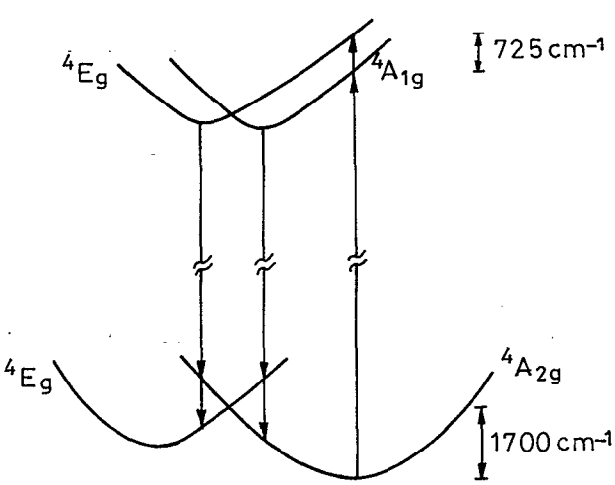

FIG. 4. Qualitative scheme for the splitting of the cubic $^4T_{1g}$ ground state and $^4T_{2g}$ excited state under a D_{3d} Jahn–Teller distortion.

Teller energy of the $^4A_{2g}$ ground state close to 1700 cm^{-1} (our result) and a splitting of the $^4A_{1g}$ and ^4E_g upper states of 725 cm^{-1} at the equilibrium geometry of the ground state, since it implies that the distortion in the upper state is much smaller than in the ground state. This is qualitatively represented in Fig. 4.

Some indication of this can be obtained from a simple model of quadratic Jahn–Teller surfaces[25,26] on the (Ω, Ω') space, which should not be taken as proof of the previous statements, but only to see that there is room for such an interpretation. If the same force constant k is adopted for both vibrational modes and the linear Jahn–Teller parameters corresponding to them are F and F', the energies of the A and E states resulting from the T ground state, relative to the minimum of this cubic state, read[26]

$$E\{A_{GS},E_{GS}\} = \frac{1}{2}k(\Omega^2+\Omega'^2) + \{2,-1\} \times \frac{1}{\sqrt{3}}(F\Omega + F'\Omega'). \quad (3)$$

A convenient rotation of the (Ω, Ω') coordinates so that the minimum of the A ground state lies in a coordinate axis, produces two new coordinates (q, q'), such that

$$E\{A_{GS},E_{GS}\} = \frac{1}{2}(q^2+q'^2) + \{2,-1\}\frac{1}{\sqrt{3}}Lq, \quad (4)$$

where $L = -\sqrt{(F^2+F'^2)/k}$, $q = (F\Omega + F'\Omega')/L$, and $q' = (F'\Omega - F\Omega')/L$. Let us now consider the excited states so that their force constant is $\lambda_k k$, their minima lie in a line which is rotated an angle θ with respect to the q axis (Fig. 5), and their linear Jahn–Teller parameter is $\lambda_L L$. Then, their energies, relative to the minimum of the cubic T excited state, are

$$E\{A_{ES},E_{ES}\} = \frac{1}{2}\lambda_k(q^2+q'^2) + \{2,-1\} \times \frac{1}{\sqrt{3}}\lambda_L L(q\cos\theta + q'\sin\theta). \quad (5)$$

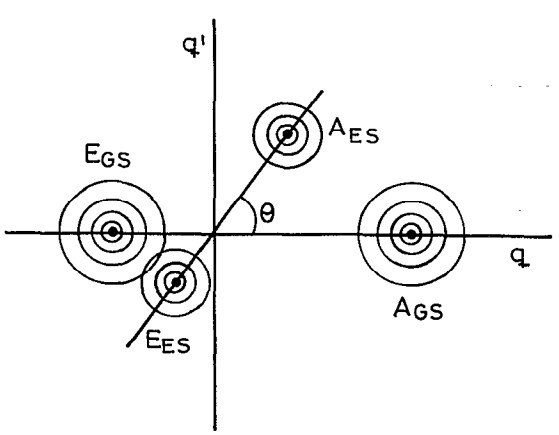

FIG. 5. Schematic representation of the locations of the ground and excited state minima on the $T\otimes(\tau_2+\tau_2')$ Jahn–Teller surface, under the assumption that the minima have D_{3d} symmetry. Each minimum is surrounded by energy isolines.

If one is interested on the differences between total electronic energies, the differences between these surfaces have to be added to the corresponding ones between the electronic energies of the cubic T ground and excited states. Simple algebra gives $L = -\sqrt{3E_{JT}(A_{GS})/2}$, where $E_{JT}(A_{GS})$ is the Jahn–Teller energy of the A ground state. Also, if we call Δ the splitting of the E_{ES} and A_{ES} at the equilibrium geometry of the ground state, we have $\Delta = 3E_{JT}(A_{GS})\lambda_L \cos\theta$. Given $E_{JT}(A_{GS})$ and Δ, the D_{3d} contributions to the total energy differences depend on two independent variables. Taking, for instance, $E_{JT}(A_{GS}) = 1700$ cm^{-1}, $\Delta = 725$ cm^{-1}, $\lambda_k = 0.6$, and $\theta = 76°$ ($\lambda_L = 0.588$), one gets D_{3d} contributions to the Stokes shifts ranging from 2700 cm^{-1} (for $A_{GS}\rightarrow A_{ES}$, $E_{GS}\leftarrow E_{ES}$) to 6000 cm^{-1} (for $A_{GS}\rightarrow E_{ES}$, $E_{GS}\leftarrow A_{ES}$). This is consistent with the very large Stokes shifts observed (from 4500 cm^{-1} in CdF_2 to 5700 cm^{-1} in BaF_2, estimated from the absorption and emission band maxima), as well as with the very large emission half-bandwidth. In addition, the D_{3d} distortion shortens by 3000 cm^{-1}, the energy difference between the E ground state and the A excited state at the equilibrium geometry of the latter, showing that the chance for a crossing of states increases considerably as a consequence of a JT-elongated distortion, this being consistent with the low emission quenching temperatures.

IV. CONCLUSIONS

The local geometry distortion induced in fluorite by Cr^+ and Cr^{3+} substitutional impurities has been studied by means of the *ab initio* environment model potential method.[9,10] Open-shell RHF plus d^n–CI has been used for the $(CrF_8)^{q-}$ ($q = 7,5$) clusters embedded in a frozen CaF_2 lattice represented by complete-ion model potentials and point-charge ions. The Cr^+ impurity induces an expansion of the surrounding cube of fluorines, while the Cr^{3+} impurity induces a D_{3d} distortion that can be described as a contraction of the cube of fluorines followed by a D_{3d} Jahn–Teller elongation; the Jahn–Teller energy being 1700 cm^{-1}. This structure is shown to be compatible with the available experimental data for Cr^{3+} defects in fluoritelike crystals.

ACKNOWLEDGMENTS

We would like to thank Professor S. Huzinaga for his interest in this work and partial support which made possible a stay at The University of Alberta. The calculations were done at the installations hosted by the Centro de Cálculo de la Universidad Autónoma de Madrid, and by the Department of Computer Services at the University of Alberta; we are very grateful to the staff of both computing services for their friendly cooperation. This work was partly supported by a grant from MEC (DGICyT PS89-0021), Spain.

APPENDIX

The adiabatic energy surface of the Jahn–Teller problem $T\otimes\tau_2$ in a cube shows, within the quadratic approximation, D_{3d} stationary points at $\xi = \eta = \zeta, \xi, \eta$, and ζ being the

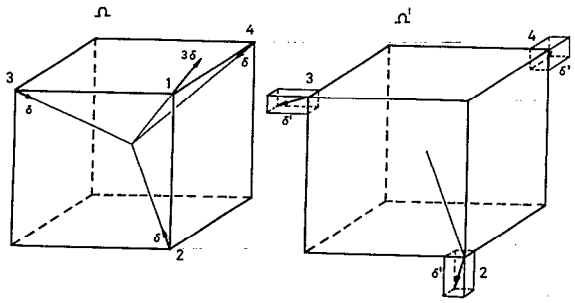

FIG. 6. D_{3d} nuclear displacement coordinates Ω and Ω'.

degenerate modes corresponding to the three τ_2 symmetry subspecies.[24,26] In the two-mode problem $T\otimes(\tau_2+\tau_2')$, the D_{3d} stationary points correspond to $\xi=\eta=\zeta$ and $\xi'=\eta'=\zeta'$. An arbitrariness exists in this case in the definition of the τ_2 and τ_2' coordinates. Here, we have chosen the coordinates described next.

Let X_i be $X_i=x_i-x_i^0$, the displacement of the fluorine nucleus i along the x axis from its cubic equilibrium position x_i^0 (Fig. 6). Equivalent definitions hold for Y_i and Z_i. By applying the projection operators corresponding to the three subspecies of the t_{2g} irreducible representation of the O_h point symmetry group[28] to X_1, Y_1, and Z_1, we have obtained:

$$\xi=\frac{1}{2\sqrt{6}}[(+X_1+Y_1+Z_1)+(-X_2-Y_2+Z_2)+(-X_3+Y_3-Z_3)+(-X_4+Y_4+Z_4)+\hat{i}],$$

$$\eta=\frac{1}{2\sqrt{6}}[(+X_1+Y_1+Z_1)+(-X_2-Y_2+Z_2)+(+X_3-Y_3+Z_3)+(+X_4-Y_4-Z_4)+\hat{i}],$$

$$\zeta=\frac{1}{2\sqrt{6}}[(+X_1+Y_1+Z_1)+(+X_2+Y_2-Z_2)+(-X_3+Y_3-Z_3)+(+X_4-Y_4-Z_4)+\hat{i}],$$

$$\xi'=\frac{1}{4\sqrt{3}}[(+2X_1-Y_1-Z_1)+(-2X_2+Y_2-Z_2)+(-2X_3-Y_3+Z_3)+(-2X_4-Y_4-Z_4)+\hat{i}],$$

$$\eta'=\frac{1}{4\sqrt{3}}[(-X_1+2Y_1-Z_1)+(X_2-2Y_2-Z_2)+(-X_3-2Y_3-Z_3)+(-X_4-2Y_4+Z_4)+\hat{i}],$$

$$\zeta'=\frac{1}{4\sqrt{3}}[(-X_1-Y_1+2Z_1)+(-X_2-Y_2-2Z_2)+(+X_3-Y_3-2Z_3)+(-X_4+Y_4-2Z_4)+\hat{i}],$$

$\hat{i}$ meaning the respective displacements of fluorine nuclei 5 to 8 which correspond to the existence of an inversion center. In order to study the surface $\xi=\eta=\zeta,\xi'=\eta'=\zeta'$, within which the D_{3d} stationary points lie, it is convenient to define the coordinates $\Omega=(\xi+\eta+\zeta)/\sqrt{3}$ and $\Omega'=(\xi'+\eta'+\zeta')/\sqrt{3}$. So, we have

$$\Omega=\frac{1}{6\sqrt{2}}[(+3X_1+3Y_1+3Z_1)+(-X_2-Y_2+Z_2)+(-X_3+Y_3-Z_3)+(+X_4-Y_4-Z_4)+\hat{i}],$$

$$\Omega'=\frac{1}{6}[(-X_2-Y_2-2Z_2)+(-X_3-2Y_3-Z_3)+(-2X_4-Y_4-Z_4)+\hat{i}],$$

which are represented in Fig. 6.

[1] *EXAFS Spectroscopy, Technique and Applications*, edited by B. K. Teo and D. C. Joy (Plenum, New York, 1981).
[2] W. Gehlhoff and W. Ulrici, Phys. Stat. Sol. **102**, 11 (1980).
[3] M. M. Zaripov, V. S. Kropotov, L. D. Livanova, and V. G. Stepanov, Fiz. Tverd. Tela (Leningrad) **9**, 209 (1967) [Sov. Phys. Solid State **9**, 155 (1967)].
[4] R. Alcalá, P. J. Alonso, V. M. Orera, and H. W. den Hartong, Phys. Rev. B **32**, 4158 (1985).
[5] S. A. Payne, L. L. Chase, and W. F. Krupke, J. Chem. Phys. **86**, 3455 (1987).
[6] K. K. Chan and L. Shields, J. Phys. C **3**, 292 (1970).
[7] R. H. Borcherts and L. L. Lohr, J. Chem. Phys. **50**, 5262 (1969).
[8] V. M. Orera, R. Alcalá, and P. J. Alonso, Solid State Commun. **58**, 79 (1986).
[9] Z. Barandiarán and L. Seijo, J. Chem. Phys. **89**, 5739 (1988).
[10] Z. Barandiarán and L. Seijo, in *Structure, Interactions, and Reactivity, Vol. 3 Condensed Matter*, edited by S. Fraga (Elsevier, Amsterdam, in press).
[11] R. McWeeny, Proc. R. Soc. London, Ser. A **253**, 242 (1959); Rev. Mod. Phys. **32**, 335 (1960); M. Kleiner and R. McWeeny, Chem. Phys. Lett. **19**, 476 (1973); R. McWeeny, *Methods of Molecular Quantum Mechanics* (Academic, London, 1989).
[12] S. Huzinaga and A. A. Cantu, J. Chem. Phys. **55**, 5543 (1971).
[13] S. Huzinaga, D. McWilliams, and A. A. Cantu, Adv. Quantum Chem. **7**, 187 (1973).
[14] S. Huzinaga, L. Seijo, Z. Barandiarán, and M. Klobukowski, J. Chem. Phys. **86**, 2132 (1987).
[15] L. Seijo, Z. Barandiarán, and S. Huzinaga, J. Chem. Phys. **91**, 7011 (1989).
[16] Z. Barandiarán, L. Seijo, and S. Huzinaga, J. Chem. Phys. **94**, 3762 (1991).
[17] H. M. Evjen, Phys. Rev. **39**, 675 (1932).
[18] R. W. G. Wyckoff, *Crystal Structures* (Wiley, New York, 1963).
[19] J. Andzelm, M. Klobukowski, E. Radzio-Andzelm, Y. Sakai, and H. Tatewaki, *Gaussian Basis Sets for Molecular Calculations*, edited by S. Huzinaga (Elsevier, Amsterdam, 1984).
[20] W. H. Adams, J. Chem. Phys. **34**, 89 (1961).
[21] P. J. Hay, J. Chem. Phys. **66**, 4377 (1977).
[22] T. H. Dunning and P. J. Hay, in *Modern Theoretical Chemistry*, edited by H. F. Schaefer III (Plenum, New York, 1977).
[23] R. Carbó and J. M. Riera, *A General SCF Theory*, Lecture Notes in Chemistry (Springer, Berlin, 1978), Vol. 5.
[24] R. Englman, *The Jahn–Teller Effect in Molecules and Crystals* (Wiley, New York, 1972).
[25] I. B. Bersuker, *The Jahn–Teller Effect and Vibronic Interactions in Modern Chemistry* (Plenum, New York, 1984).
[26] L. K. Aminov and B. Z. Malkin, Fiz. Tverd. Tela (Leningrad) **9**, 1316 (1967) [Sov. Phys. Solid State **9**, 1030 (1967)].
[27] S. Y. Shaskin and W. A. Goddard III, Phys. Rev. B **33**, 1353 (1986).
[28] F. A. Cotton, *Chemical Applications of Group Theory* (Wiley, New York, 1971).